Journal of Biomedical Optics

BiomedicalOptics.SPIEDigitalLibrary.org

# Resonance Raman enhancement optimization in the visible range by selecting different excitation wavelengths

Zhong Wang
Yuee Li

SPIE.

# Resonance Raman enhancement optimization in the visible range by selecting different excitation wavelengths

**Zhong Wang and Yuee Li***
Lanzhou University, School of Information Science and Engineering, 222 Tianshui South Road, Lanzhou 730000, China

**Abstract.** Resonance enhancement of Raman spectroscopy (RS) has been used to significantly improve the sensitivity and selectivity of detection for specific components in complicated environments. Resonance RS gives more insight into the biochemical structure and reactivity. In this field, selecting a proper excitation wavelength to achieve optimal resonance enhancement is vital for the study of an individual chemical/biological ingredient with a particular absorption characteristic. Raman spectra of three azo derivatives with absorption spectra in the visible range are studied under the same experimental conditions at 488, 532, and 633 nm excitations. Universal laws in the visible range have been concluded by analyzing resonance Raman (RR) spectra of samples. The long wavelength edge of the absorption spectrum is a better choice for intense enhancement and the integrity of a Raman signal. The obtained results are valuable for applying RR for the selective detection of biochemical constituents whose electronic transitions take place at energies corresponding to the visible spectra, which is much friendlier to biologial samples compared to ultraviolet.  [DOI: 10.1117/1.JBO.20.9.095003]

Keywords: resonance Raman spectroscopy; excitation wavelength; visible absorption spectra; enhancement factor.

Paper 150398R received Jun. 18, 2015; accepted for publication Aug. 5, 2015; published online Sep. 3, 2015.

## 1 Introduction

Raman spectroscopy (RS) is based on the inelastic scattering of radiation by the sample and has been employed to detect and identify constituents in numerous chemical and biological fields.[1] Resonance Raman spectroscopy (RRS) has significantly enhanced sensitivity and selectivity compared with normal RS due to the overlap of the excitation wavelength and the electronic transition, which permits selectively analyzing relatively few molecules in a complicated system and extends the utility of the Raman scattering technique.[2] Therefore, RRS has been broadly applied for studying DNA, RNA, and protein interactions for the label-free Raman methods in the bioanalytical and life sciences field.[3–6] UV-RRS has been long employed to gain insight into the biomolecular properties of cells[7,8] since the absorption spectra of most biological assemblies including DNA, RNA, and protein are located in theUV range.

Thanks to the lower energy of photons, a visible laser is friendlier for biological samples. Applications of visible-RRS is growing for analyzing biomolecules with an electronic transition in the visible part of spectrum such as carotenoids[9–12] and hemes.[13] For these studies, the judicious choice of excitation wavelength is essential for optimal sensitivity and selectivity of the molecular species of interest in a complex environment or as part of a very large molecule. However, many laser systems still suffer from the lack of tuning ability and the Raman detection system will be more complex because specific filters are needed for the collection of a Raman spectrum even though tunable lasers are available. Furthermore, the Raman signal is sometimes overwhelmed by its fluorescence background because of the electronic absorption which provides the enhancement mechanism. Under certain excitation, we achieve intense resonance enhancement of some specific molecules, but vibrations that undergo little or no enhancement are likely to become invisible in the spectrum because of the strong background induced by the RRS mechanism. This results in decreased information content of the Raman spectrum and impedes the combination of RRS and normal RS. In other words, we have to consider a trade-off between sensitivity and information enrichment. Therefore, we expect that resonance enhancement for Raman bands of different molecules with a specific absorption spectrum can be predicted by theoretical approaches or experience-based laws. On one hand, the Raman measurement system can be simplified by using fixed lasers; on the other hand, the excitation wavelength can be properly arranged for obtaining important spectra information from complex molecules by combining RRS and normal RS. Multiple excitation wavelengths can also be used for improving detection specificity due to the strong dependence on the excitation wavelength of the resonance Raman signal. Yellampalle et al.[14–16] proposed a multiple excitation wavelengths' DUV resonance Raman technique for the detection of several explosives which provides a unique signature improving specificity.

In this paper, by introducing a dialkyl amino electron donor and different amounts of nitrile group electron acceptors, three derivatives including azo Am-CN, azo Am-2CN, and azo Am-3CN are synthetized. Strong intramolecular charge transfer leads to the significant red-shift of the electronic absorption

*Address all correspondence to: Yuee Li, E-mail: liyuee@lzu.edu.cn

1083-3668/2015/$25.00 © 2015 SPIE

spectra, so these three derivatives have absorption spectra ranging from 350 to 700 nm. Resonance Raman cross-sections and the absorption of both the excitation and scattered light depend strongly on the excitation wavelength. Therefore, Raman band intensities depend on the excitation wavelength in a complex way. Here, resonance enhancement dependency on absorption characteristics at the excitation wavelength has been explored by processing and analyzing measured RR spectra of these three derivatives at the designed Raman measurement setup equipped with 488, 532, and 633 nm lasers.

## 2 Methods

### 2.1 *Raman Spectra Measurements*

RS was performed using an Alpha SNOM confocal Raman microscope system (WITec, Germany) equipped with 488 nm (JDSU FCD488), 532 nm (Coherent Verdi V-6), and 633 nm He–Ne lasers (Coherent) as laser sources for excitation, and an ACTON 300i spectrometer (Princeton Instruments, Trenton, New Jersey) for Raman spectra detection. The laser beam was focused into the sample by a Plan Apo 60× oil immersion objective lens with NA = 1.4 (Nikon, Japan). Raman spectra of solutions were acquired with an integration time of 1 s/pixel and averaged over the area of $8 \times 8$ pixels. It is well-known that the Raman scattering cross-section is proportional to $\lambda^{-4}$ and the response of the CCD detector varies with the wavelenth of the identified optical signal. Therefore, all Raman spectra of samples have been normalized to the Raman intensity of the solvent [dimethyl sulfoxide (DMSO)] to remove the Raman intensities variations caused by response parameters and the Raman scattering cross-section change with the excitation wavelength.

### 2.2 *Structures of Three Derivatives and Normalized Absorption Spectra*

Different auxochromes were attached to the chromophore to modify the ability of that chromophore to absorb light, and three derivatives including azo Am-CN, azo Am-2CN, and azo Am-3CN were synthetized following a modified procedure as described in the literature.[17] They have different absorption spectra in the visible wavelengths ranging from blue to red (400 to 700 nm) [Figs. 1(a) and 1(b)].

### 2.3 *Resonance Raman Intensity and the Enhancement Factor*

Three azo derivatives are diluted in DMSO with the same concentration of 670 $\mu$M which is much lower than 5 mM (the detection limit for traditional Raman detection). The available 488, 532, and 633 nm lasers are used for the excitation of Raman scattering and Raman spectra are obtained with the same confocal microscope under the same experimental conditions (room temperature, laser power after objective, accumulation time).

We measured the Raman intensity of the azo-benzene DMSO solution with a 670 $\mu$M × 100 concentration under the same experimental conditions (as shown in Table 1 and Fig. 2). Because of the resonance enhancement contribution by a tiny absorption difference at three excitation wavelengths, we observed insignificant differences at three excitations. Then we chose the Raman intensity of azo-benzene at 1436 $cm^{-1}$ [$\nu$(N=N)] under the 633-nm excitation, which is far away from the UV absorption spectrum of azo-benzene, as a standard for evaluating the enhancement and estimated enhancement factors (EFs) that are listed for different excitations.

RRS is due to the overlap of the excitation wavelength and absorption spectra of measured samples and Raman scattering can be enhanced by resonance, but Raman scattering may also be reabsorbed if the absorption of the measured sample is still strong enough at the wavelength of the Raman scattering signal. Therefore, the final enhanced Raman intensity is a product of resonant enhancement and reabsorption of Raman scattering. Where should we choose our excitation wavelength for optimum resonance enhancement of the Raman intensity? The short wavelength ridge, the long wavelength ridge, or the maximum point of the absorption curves? In order to consider the influence of reabsorption of the Raman scattering by the measured results, the Raman spectra of three derivatives were drawn in two figures: the first figure uses a Raman shift ($cm^{-1}$) as the horizontal coordinate, from which we can analyze the Raman shift intensity of specific chemical bands; the second figure

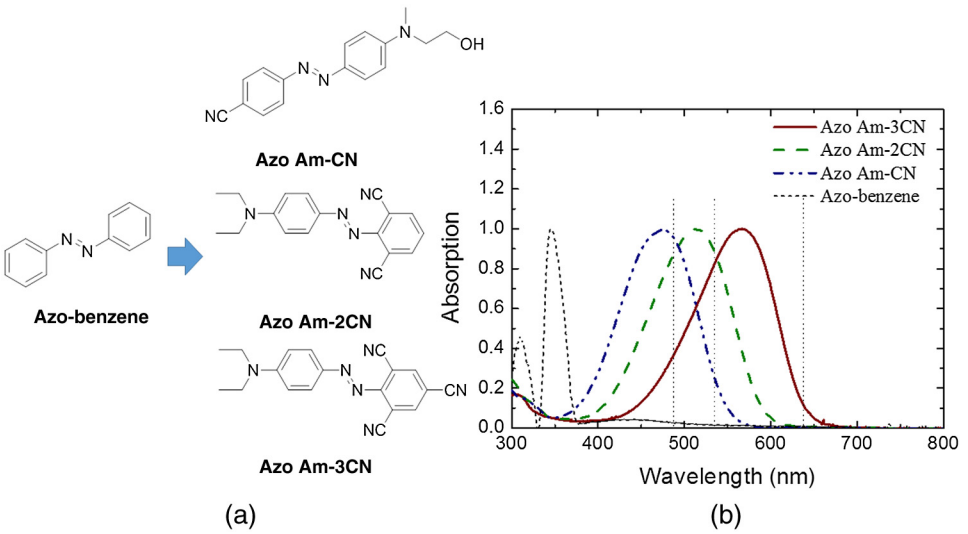


**Fig. 1** (a) Chemical structures and (b) normalized absorption spectra of azo-benzene, azo Am-CN, azo Am-2CN, and azo Am-3CN.

**Table 1** Raman intensities of azo-benzene at 488, 532, and 633 nm laser excitation (concentration: 670 $\mu$M × 100).

| Excitation wavelength | Absorption of azo-benzene | Raman intensities of azo-benzene ~1436 cm$^{-1}$ |
|---|---|---|
| 488 nm | 0.026 | 1261 |
| 532 nm | 0.014 | 908 |
| 633 nm | 0.008 | 514 |

uses the practically measured wavelength of a Raman scattering signal as the horizontal coordinate, and the absorption spectra are combined to evaluate the Raman intensity decline caused by the sample reabsorption of Raman scattering.

## 3 Results

Three intense Raman peaks of azo Am-CN are observed at 1135, 1375, and 1600 cm$^{-1}$ [Fig. 3(a)] and intensities are listed in Table 2. The EFs are calculated by dividing the Raman peaks of the main structure [$\nu$(N=N)] at 1375 cm$^{-1}$ by that of azo-benzene at 1435 cm$^{-1}$ (as shown in Table 1 and Fig. 2. No Raman signal of azo-benzene was observed in solution with the 670 $\mu$M concentration]. Three derivatives have EFs ranging from 10 to $10^3$ at different excitations. Assignments of Raman bands have been done according to theoretical analysis[18] and marked in Fig. 3(a). Obtained results indicate that: (a) Raman intensities at 1135, 1375, and 1600 cm$^{-1}$ are enhanced due to a resonance mechanism at all three excitations; (b) Raman intensity increases, but not proportionally, when the absorption increases. Figure 3(b) gives all Raman scattering signals versus the real wavelength under three excitations. Three excitation wavelengths are located at the long wavelength ridge of the absorption spectrum of azo Am-CN. In this case, the real wavelength of the Raman peaks with a smaller Raman shift is close to the peak of the absorption spectrum, so Raman enhancement for peaks with a smaller Raman shift show a gentler increase due to the reabsorption of Raman scattering by the azo Am-CN sample (for example: when absorption increases from 0.293 to 0.95, the intensity of the 1135 cm$^{-1}$ peak has little change while those of 1375 and 1600 cm$^{-1}$ double).

In the case of the azo Am-2CN sample, three intense Raman peaks are observed at 1135, 1375, and 1600 cm$^{-1}$ [Fig. 4(a)] and the intensities are listed in Table 3. The absorption spectrum of azo Am-2CN [solid curve, Fig. 4(b)] shows that the maximum absorption occurs at 514 nm and one excitation wavelength is located at the short wavelength ridge of the absorption spectrum of azo Am-2CN and the other two excitations are located at the long wavelength ridge. Azo Am-2CN has a similar amount of absorption at 488 and 532 nm excitations. Results indicate that: (a) Raman intensities of the two peaks at 1375 and 1600 cm$^{-1}$ are enhanced due to the resonance mechanism; (b) Raman intensity increases with the increase of the absorption, and when the excitation wavelength is close to the maximum absorption wavelength, the absorption dominates for the resonance enhancement and the reabsorption shows a limited influence (e.g., when we move the excitation from 488 to 532 nm, the absorption increases slightly from 0.873 to 0.913 and the Raman intensities of the 1375 and 1600 cm$^{-1}$ peaks have similar growths. The reabsorption has

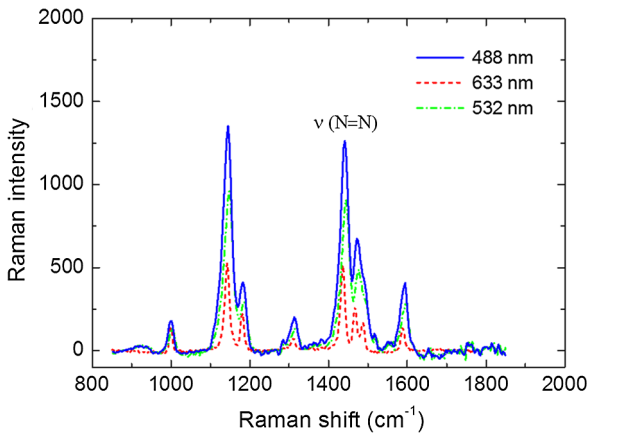


**Fig. 2** Raman spectra of azo-benzene at 488, 532, and 633 nm excitations, (power: 5 mW, accumulation time: 1 s, concentration: 67 mM in DMSO).

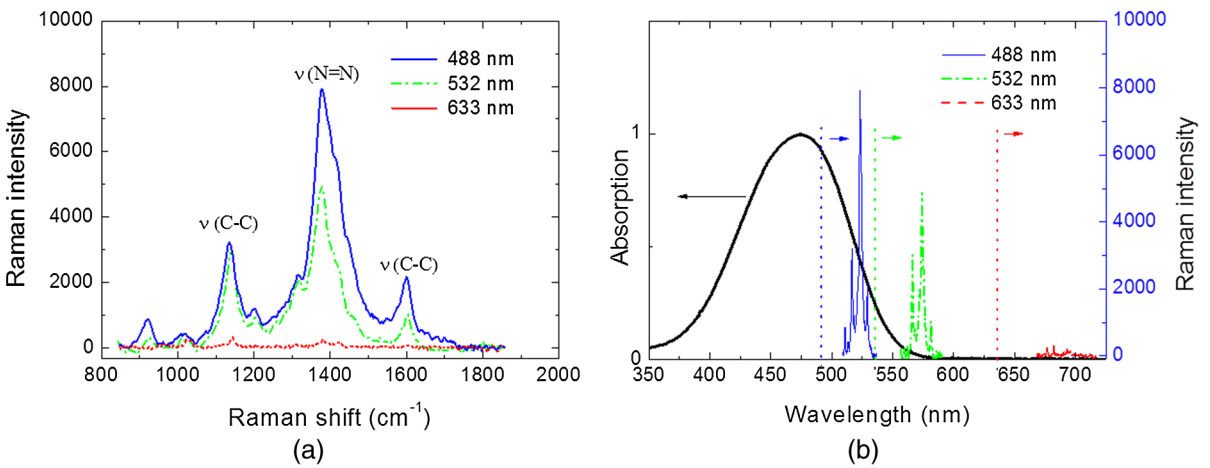


**Fig. 3** Raman spectra of azo Am-CN at 488, 532, and 633 nm excitations (power: 5 mW, accumulation time: 1 s, concentration: 670 $\mu$M in DMSO): (a) standard Raman spectra versus Raman shift (cm$^{-1}$) and (b) Raman spectra versus the measured wavelength of Raman scattering signal combined with the absorption spectra of azo Am-CN.

**Table 2** Raman intensities of azo Am-CN at 488, 532, and 633 nm laser excitation (concentration: 670 $\mu$M).

| Excitation wavelength | Absorption | Raman intensities | | | Estimated enhancement factor (EF) |
|---|---|---|---|---|---|
| | | 1135 cm$^{-1}$ [$\nu$(C—C)] | 1375 cm$^{-1}$ [$\nu$(N=N)] | 1600 cm$^{-1}$ [$\nu$(C—C)] | |
| 488 nm | 0.95 | 3222 | 7913 | 2174 | 1539 |
| 532 nm | 0.293 | 3010 | 4973 | 1042 | 967.5 |
| 633 nm | 0.0013 | 341 | 235 | 70 | 45.7 |

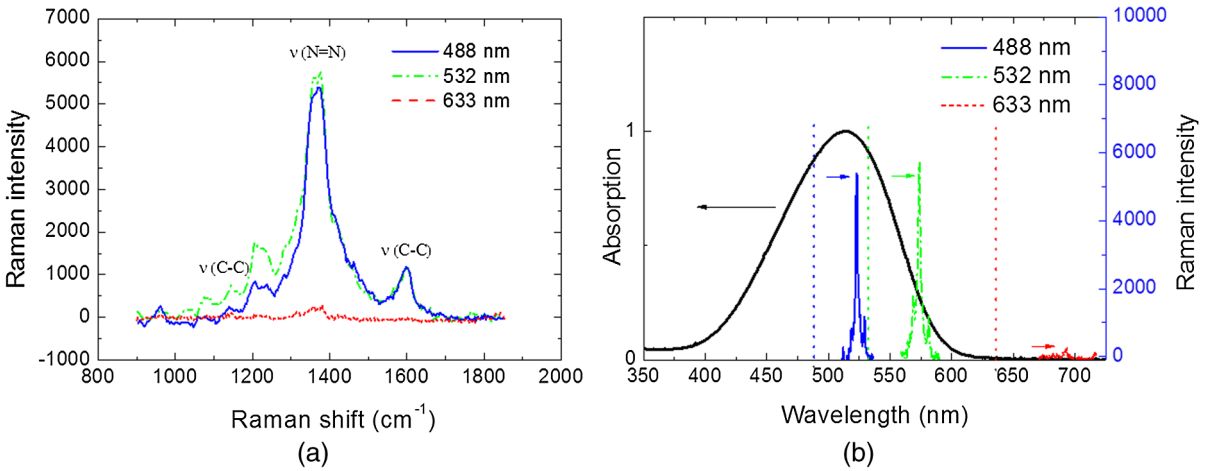


**Fig. 4** Raman spectra of azo Am-2CN at 488, 532, and 633 nm excitations (power: 5 mW, accumulation time: 1 s, concentration: 670 $\mu$M in DMSO): (a) standard Raman spectra versus Raman shift (cm$^{-1}$) and (b) Raman spectra versus the measured wavelength of Raman scattering signal combined with the absorption spectra of azo Am-2CN.

little influence although the real wavelength of the Raman scattering signal at 488-nm excitation is much closer to the maximum absorption wavelength than that at 532 nm and should be more susceptible to the reabsorption of the samples).

In the case of azo Am-3CN, three intense Raman peaks are observed at 1135, 1375, and 1600 cm$^{-1}$ [Fig. 5(a)] and the intensities are listed in Table 4. 488 and 532 nm excitations are located at the short wavelength ridge of the absorption spectrum and the 633-nm excitation is located at the long wavelength ridge [Fig. 5(b)]. Results indicate that: (a) Raman intensities of the two peaks at 1375 and 1600 cm$^{-1}$ are enhanced due to the resonance mechanism; (b) by comparing Raman intensities of this sample at 488 and 633 nm, we can conclude that the enhanced Raman bands at the 488-nm excitation (far from the maximum absorption wavelength) are influenced by reabsorption since more than double absorption the at 488 nm did not cause a doubling of the intensity of the Raman bands at 1600 cm$^{-1}$. However, when the excitation moved from 488 to 532 nm, the double absorption leads to a 3× times increase in the intensities at 1375 and 1600 cm$^{-1}$ because 532 nm is close to the maximum absorption wavelength and the absorption dominates for Raman enhancement, which confirms the conclusion from the azo Am-2CN sample.

In brief, due to optical absorption at excitation, these three derivatives generate strong signals to improve a concentration detection threshold to <100 $\mu$M at 488, 532, and 633 nm excitation lines.

**Table 3** Raman Intensities of azo Am-2CN at 488, 532, and 633 nm laser excitation (concentration: 670 $\mu$M).

| Excitation wavelength | Absorption | Raman intensities | | | Estimated enhancement factor |
|---|---|---|---|---|---|
| | | 1135 cm$^{-1}$ [$\nu$(C—C)] | 1375 cm$^{-1}$ [$\nu$(N=N)] | 1600 cm$^{-1}$ [$\nu$(C—C)] | |
| 488 nm | 0.873 | 262 | 5377 | 1134 | 1046 |
| 532 nm | 0.913 | 745 | 5778 | 1210 | 1124 |
| 633 nm | 0.006 | 87 | 300 | 40 | 58.3 |

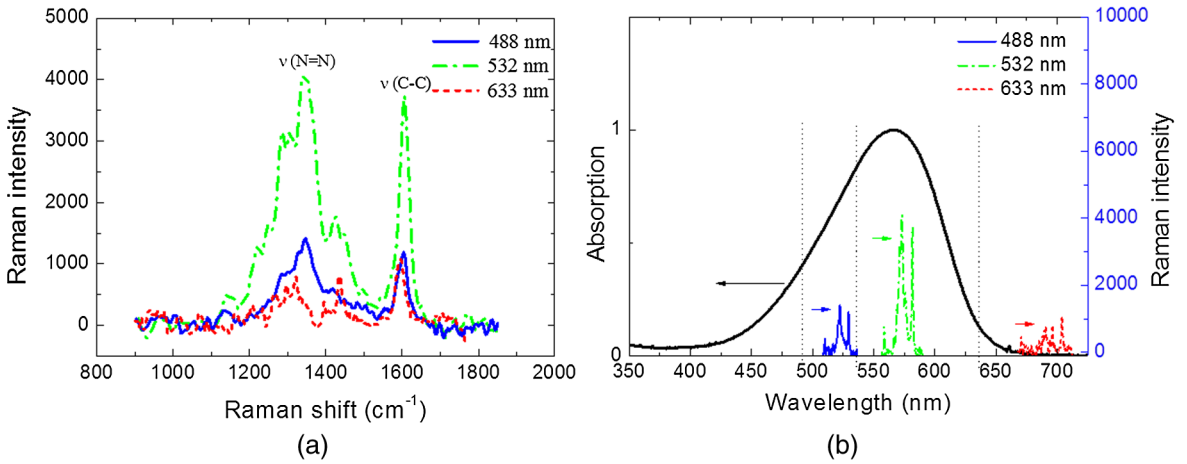


**Fig. 5** Raman spectra of azo Am-3CN at 488, 532, and 633-nm excitations (power: 5 mW, accumulation time: 1 s, concentration: 670 $\mu$M in DMSO): (a) standard Raman spectra versus Raman shift ($cm^{-1}$) and (b) Raman spectra versus the measured wavelength of Raman scattering signal combined with the absorption spectra of azo Am-3CN.

**Table 4** Raman intensities of azo Am-3CN at 488, 532, and 633-nm laser excitation (concentration: 670 $\mu$M).

| Excitation wavelength | Absorption | Raman intensities | | Estimated enhancement factor |
|---|---|---|---|---|
| | | ~1375 $cm^{-1}$ [$\nu$(N=N)] | ~1600 $cm^{-1}$ [$\nu$(C–C)] | |
| 488 nm | 0.369 | 1470 | 1207 | 286 |
| 532 nm | 0.794 | 4096 | 3803 | 797 |
| 633 nm | 0.1584 | 775 | 1160 | 150.8 |

## 4 Discussion

The positive contribution of the electronic transition for resonance Raman enhancement beats the negative contribution of the reabsorption of Raman scattering by the sample for all samples, but we need to consider this negative contribution for specific Raman bands. To summarize: (a) resonance Raman intensity obviously climbs with the growth of the absorption of samples at the short ridge of the absorption spectrum [azo Am-3CN, the Raman intensity had an around three times increase from 1470 to 4096 when the excitation changed from 488 nm (Ab: 0.369) to 532 nm (Ab: 0.794)]; (b) resonance Raman intensity declines slowly with the lessening of the absorption at the long ridge of the absorption spectrum [azo Am-CN, the Raman intensity had a change from 7913 to 4973 when the excitation wavelength changed from 488 nm (Ab: 0.95) to 532 nm (Ab: 0.293, three times decrease)]; (c) resonance Raman intensity has a ~20-times decline when the absorption has ~100 times decrease (Fig. 4). This magnitude difference is enough for distinguishing two different components in a complex system; (d) even at the edge of the curve of absorption with only 0.0013 of the maximum, the resonance has a 10 ~ 100 enhancement contribution to the Raman intensity; (e) a ~60 $cm^{-1}$ blue-shift (from ~1436 to ~1375 $cm^{-1}$) of the Raman line was observed for the same chemical band after gaining enhancement and the enhanced Raman bands become broader.

## 5 Conclusions

The main focus of this work was to determine experiential laws of the resonance enhancement factor with the excitation wavelength, especially in the visible range. By processing and analyzing resonance Raman spectra of three derivatives of azo-benzene, we obtained the enhancement factor tendency with the excitation wavelenth at two ridges of the absorption spectrum. We concluded that the long wavelength edge of the absorption spectrum works better for Raman enhancement. With the same value of the normalized absorption, the longer wavelength shows a more intense Raman enhancement and a more complete Raman spectrum. The results are valuable for the application of RRS-based selective components analysis in complex biological systems and the design of numerous resonance Raman reporters that are suitable for chemical and biological fields.

### *Acknowledgments*

The authors thank Dr. Jeongyun Heo at Institute for Laser, Photonics, Biophotonics for providing four samples for experimental requirements. This work was supported by National Natural Science Foundation of China (No. 61405083), the Fundamental Research Funds for the Central Universities (Nos. lzujbky-2013-187, lzujbky-2013-42), and China Scholarship Council.

### *References*

1. H. Abramczyk and B. Brozek-Pluska, "Raman imaging in biochemical and biomedical applications. diagnosis and treatment of breast cancer," *Chem. Rev.* **113**(8), 5766–5781 (2013).
2. J. R. Ferraro, K. Nakamoto, and C. W. Brown, *Introductory Raman Spectroscopy*, Academic Press, Amsterdam, Boston, p. 1 online resource (xiii, pp. 434) (2003).
3. D. Gill, R. G. Kilponen, and L. Rimai, "Resonance Raman scattering of laser radiation by vibrational modes of carotenoid pigment molecules in intact plant tissues," *Nature* **227**(5259), 743–744 (1970).
4. E. V. Efremov, F. Ariese, and C. Gooijer, "Achievements in resonance Raman spectroscopy: review of a technique with a distinct analytical chemistry potential," *Anal. Chim. Acta* **606**(2), 119–134 (2008).
5. L. Wei et al., "Live-cell imaging of alkyne-tagged small biomolecules by stimulated Raman scattering," *Nat. Methods* **11**(4), 410–412 (2014).

6. M. Ibrahim, C. Xu, and T. G. Spiro, "Differential sensing of protein influences by NO and CO vibrations in heme adducts," *J. Am. Chem. Soc.* **128**(51), 16834–16845 (2006).
7. S. A. Oladepo et al., "UV resonance Raman investigations of peptide and protein structure and dynamics," *Chem. Rev.* **112**(5), 2604–2628 (2012).
8. K. Faulds, W. E. Smith, and D. Graham, "Evaluation of surface-enhanced resonance Raman scattering for quantitative DNA analysis," *Anal. Chem.* **76**(2), 412–417 (2004).
9. P. Bhosale et al., "Resonance Raman quantification of nutritionally important carotenoids in fruits, vegetables, and their juices in comparison to high-pressure liquid chromatography analysis," *J. Agric. Food Chem.* **52**(11), 3281–3285 (2004).
10. I. V. Ermakov et al., "Resonance Raman detection of carotenoid antioxidants in living human tissue," *J. Biomed. Opt.* **10**(6), 064028 (2005).
11. I. V. Ermakov and W. Gellermann, "Optical detection methods for carotenoids in human skin," *Arch. Biochem. Biophys.* **572**, 101–111 (2015).
12. S. T. Mayne et al., "Resonance Raman spectroscopic evaluation of skin carotenoids as a biomarker of carotenoid status for human studies," *Arch. Biochem. Biophys.* **539**(2), 163–170 (2013).
13. F. Adar, S. N. Dixit, and M. Erecinska, "Resonance Raman spectra of cytochromes c and b in Paracoccus denitrificans membranes: evidence for heme–heme interactions," *Biochemistry* **20**(26), 7528–7531 (1981).
14. B. Yellampalle et al., "Multiple-excitation-wavelength resonance-Raman explosives detection," *Proc. SPIE* **8018**, 801819 (2011).
15. B. Yellampalle et al., "High-sensitivity explosives detection using dual-excitation-wavelength resonance-Raman detector," *Proc. SPIE* **9073**, 90730H (2014).
16. B. Yellampalle, "Explosive sensing using multiple-excitation-wavelength resonance-Raman scattering," in *2011 Conf. on Lasers and Electro-Optics (Cleo)* (2011).
17. C. L. Weeks et al., "Investigation of an unnatural amino acid for use as a resonance Raman probe: Detection limits, solvent and temperature dependence of the nuC identical withN band of 4-cyanophenylalanine," *J. Raman Spectrosc.* **39**(11), 1606–1613 (2008).
18. N. Biswas and S. Umapathy, "Structures, vibrational frequencies, and normal modes of substituted azo dyes: infrared, Raman, and density functional calculations," *J. Phys. Chem. A* **104**(12), 2734–2745 (2000).



**Zhong Wang** has been engaged in university education and research in Lanzhou University since 2004. His current research interests include data analysis of Raman spectrum and data mining in biological field.

**Yuee Li** received her doctoral degree in 2010. She has been engaged in university education and research work in Lanzhou University since 2004 and has published about 20 papers. Her current research interests include resonance Raman, plasmonics, and application of nanophotonics in the biochemical field.